Glass and Ceramics, Vol. 68, Nos. 1 – 2, May, 2011 (Russian Original, Nos. 1 – 2, January – February, 2011)

UDC 666.3-492:666.762.1

INTERRELATION OF MORPHOLOGICAL FEATURES OF $ZrO_2 - CeO_2$ NANOPOWDERS WITH CERAMIC CHARACTERISTICS

L. I. Podzorova,[1, 2] A. A. Il'icheva,[1] O. I. Pen'kova,[1] S. V. Kutsev,[1] N. A. Alad'ev,[1] and L. I. Shvorneva[1]

Translated from *Steklo i Keramika*, No. 1, pp. 17 – 20, January, 2011.

The dimensional and morphological parameters of $ZrO_2 - CeO_2$ nanopowders obtained from carbonate and hydroxide precursors have been investigated. The effect of the nature of the precipitating agent and the heat-treatment temperature on the morphology of the synthesized powders, their degree of agglomeration, and the porous structure is shown. The differences found in the degree of structuring of the powders affect the sintering process and the production of samples with different degrees of compaction.

Key words: sol-gel, nanopowders, morphology, ceramics.

As a rule, refractory oxide ceramic powders sinter by means of volume of diffusion whose characteristics are described by two basic factors: the diffusion coefficient and the sizes of the sintering particles [1, 2].

The use of the initial nanopowders in ceramics technology has an intensifying effect on the sintering process; this effect is due to the size factor which determines the simultaneous increase of the contact zones and the gradient of the diffusion coefficient [2]. In addition, the final sintering temperature decreases because the melting point of fine particles decreases according to Kelvin's equation [1].

Highly disperse systems, possessing excess surface energy, strive to dissipate the energy by forming agglomerates or aggregates of individual particles [2 – 4], which lowers the sintering "activity" of powders.

The degree of agglomeration and the structure and properties of the aggregates depend on the methods used to obtain the powders. When precursors are obtained by liquid-phase synthesis, the structure of the intermediate compounds is inherited: various factors affect the formation of these compounds: the rate of precipitation, the concentration and nature of the precipitated components and precipitator, the pH of the medium, the temperature, and other factors [3 – 5]. The first aggregates to form become stronger and increase in size under the subsequent heat treatment. Lowering the heat-treatment temperature for the precursors is one way to decrease the degree of agglomeration.

[1] Institution of the Russian Academy of Sciences (RAS), A. A. Baikov Institute of Metallurgy and Materials Science of RAS, Moscow, Russia.

[2] E-mail: podzorova@pochta.ru.

The results of an investigation of the effect of precipitators ammonium hydroxide, urotopine (hexametylene tetraamine) $(CH_2)_6N_4$, and carbamide $(NH_2)_2CO$, on the production of nanopowders in the systems $ZrO_2 - Y_2O_3$ and $ZrO_2 - CeO_2$ are presented in [6 – 8]. It is show that powders which are most active with respect to sintering are obtained by using ammonium hydroxide as the precipitator.

It is indicated in [2] that carbonate precursors of powders usually crystallize at a lower temperature than the hydroxides of definite components. It can be supposed that nanopowders obtained from carbonate and hydroxide precursors will possess a different morphology.

In this connection, the objective of the present work became the study of the effect of the size and morphological characteristics of $ZrO_2 - CeO_2$ nanopowders obtained from carbonate and hydroxide precursors on the process of their sintering.

For this investigation, the following composition (mol.%) was chosen: $88ZrO_2 + 12CeO_2$, which makes it possible to stabilize the tetragonal modification ZrO_2 [8].

Nanopowders were obtained from precursors synthesized by the sol-gel method as follows:

sample 1) reverse precipitation using ammonium hydroxide;

sample 2) reverse precipitation using ammonium carbonate;

sample 3) direct precipitation using ammonium carbonate.

For synthesis, 1 M salt solutions $ZrOCl_2 \cdot 8H_2O$ and $Ce(NO_3)_3 \cdot 6H_2O$ and solvent solutions 6H $NH_3 \cdot H_2O$ and 20% $(NH_4)_2CO_3$ were used. Isobutane C_4H_7OH was used as an SAS.

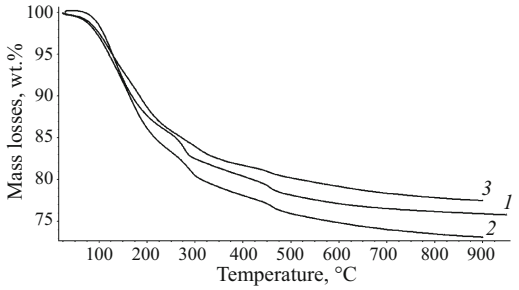

Fig. 1. Mass losses in the temperature range 100 – 900°C for samples 1, 2, and 3.

The precipitation products (xerogels) obtained after drying were heat-treated at 650 and 950°C.

Samples with the dimensions 4 × 4 × 32 mm were formed by semidry pressing at specific pressure 200 MPa.

The sintering was conducted at temperatures 1400 – 1500°C in electric furnaces with lanthanum chromite in air.

The following methods were used to investigate the synthesized materials.

The completeness of the precipitation of the components was determined by means of elemental analysis of precursors by the method of emission spectrometry with inductively coupled plasma using an ULTIMA-2 spectrometer [5].

Thermogravimetric analysis was performed on a NETZSCH STA 409 PC/PG simultaneous thermal analyzer with dynamic heating at the rate 15 K/min.

A qualitative analysis of the phase composition of the samples was performed with an XRD-600 diffractometer (Shimadzu Company) in CuK_α radiation (λ = 1.54 Å) in the angular interval $2\theta = 26 – 36°$, which corresponds to the region of the main reflections for cubic, monoclinic, and tetragonal modifications of ZrO_2. Data from the international standards bank (JCPDS) were used to identify solid solutions based on zirconium dioxide.

The specific surface area of the powders was measured using a TriStar-3000 adsorption-structure analyzer. The results of the analysis were used to determine the differential and integral dependence of the pore volume distribution versus the pore diameter.

The quantitative composition of the agglomerates of the powders was determined with an Annnilizette-22 analyzer.

TABLE 1. Mass Content of Oxides in Synthesized Powders

Oxide	Content in powders, wt.%			
	Theoretical	Computed*		
		1	2	3
ZrO_2	84.0	82.9	81.9	82.5
CeO_2	16.0	17.1	18.1	17.5

* Error no more than 2 wt.%. The main impurity element in the powders 1, 2, 3 is irremovable hafnium in amounts ranging from 1 to 1.3 wt.%.

The photographs of the powder morphology were obtained with a JSM-7401F scanning electron microscope and photographs of the microstructure samples were obtained with a LEO 1420 scanning electron microscope.

The relative density and porosity of the sintered ceramic samples was determined by hydrostatic weighing.

Elemental analysis of the precursors was used as a basis for calculating the content of the main oxides, presented in Table 1 and confirming the high precipitation density of the components and the conformance to the prescribed composition.

Figure 1 displays the results of the thermogravimetric analysis of the precursors, showing that the mass losses of the samples stabilize during heat-treatment above 600°C.

Taking this fact into account, the powders were obtained after heat treatment at the temperatures 650 and 950°C.

The crystallinity of the main crystalline phase represented by a solid solution based on ZrO_2 is a function of the heat-treatment temperature of the precipitation products. The specific surface area S_{sp} of the corresponding powders correlates with their crystallinity. Comparative data are presented in Table 2.

The precipitation products after heat-treatment consist of a powder with individual particle sizes from 70 to 22 nm, and crystallinity from 52 to 100%.

The powders 2 and 3 heat-treated at 650°C (2/650 and 3/650) and the powder 1 heat-treated at 950°C (1/950) have close size characteristics.

A change of the conditions of synthesis of precursors (precipitators of various kinds and method of precipitation) determines not only the dimensional but also the morphological characteristics of the synthesized nanopowders. The porous structure of the powders chosen is represented by the integral and differential relations in Fig. 2.

The total porosity of the powders is close: for 1/950 — 0.15, for 2/650 — 0.18, for 3/650 — 0.16 cm^3/g. However, the components of the total porosity have different dimensional characteristics. Pores of size 15 nm predominate in 2/650 and 3/650 powders and 20 nm in 1/950 powders. Fine pores around 3 nm in size are present in 2/650 and 3/650 powders, and their content is higher than in 3/650 powder.

TABLE 2. Crystallinity of the Main Crystalline Phase and Size Characteristics of the Synthesized Powders

Sample	Heat treatment, °C					
	650			950		
	crystallinity, %	S_{sp}, m^2/g	particle size, nm	crystallinity, %	S_{sp}, m^2/g	particle size, nm
1	52	40	22	60	27	36
2	63	33	30	90	14	60
3*	64	30	32	100	12	70

* Sample 3, heat-treated at 950°C, was chosen as the standard.

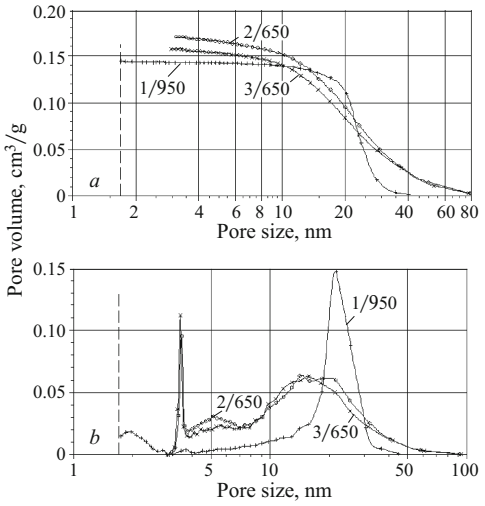

Fig. 2. Integral (*a*) and differential (*b*) curves of the pore-volume distribution in the range of mesopores from their diameter in the synthesized powders 1/950, 2/650, and 3/650.

Synthesized nanopowders comprise a system of agglomerates, and the agglomerate-size distribution is various (Fig. 3). The powder 1/950 is represented by agglomerates from 1 to 300 nm, 1/260 — from 0.5 to 90 nm, and 3/650 — from 0.5 to 60 nm. The powder 1/950 is comprised of 25% agglomerates to 10 nm, and the powders 2/650 and 3/650 are each comprised of about 60% such agglomerates.

The powder 3/650 is represented by agglomerates with can be characterized as dense formations in contrast to the agglomerates of the powders 1/950 and 2/650, which are represented by "loose" components. The electronic photographs in Fig. 4 illustrate this circumstance.

The samples obtained after formed powders were sintered at 1400 – 1500°C under identical conditions had different relative density ρ and closed porosity P_{closed}, which is represented in Table 3.

It would appear that compaction of samples with close specific surface area should be practically identical, but this behavior is not observed. The samples sintered from powder No. 2/650, in which the specific area is highest in this series, have a relative density that is less than that of samples 3/650 and correspondingly at 1400°C — 97.1 and 96.2% and at 1500°C — 99.2 and 98.7%.

The grain composition of the microstructure of the corresponding ceramics depends on the sizes of the individual powder particles. The grain size in a ceramic sintered at 1450°C ranges from 400 to 800 nm, and regions with sizes above 800 nm corresponding to the depletion of melted fine particles are observed; Fig. 5 illustrates this.

Since pores smaller than 5 nm are most numerous in 2/650 and 3/650 powders and are extremely difficult to remove during sintering [2, 8], a substantial closed porosity remains in the corresponding ceramic with the sintering regimes used.

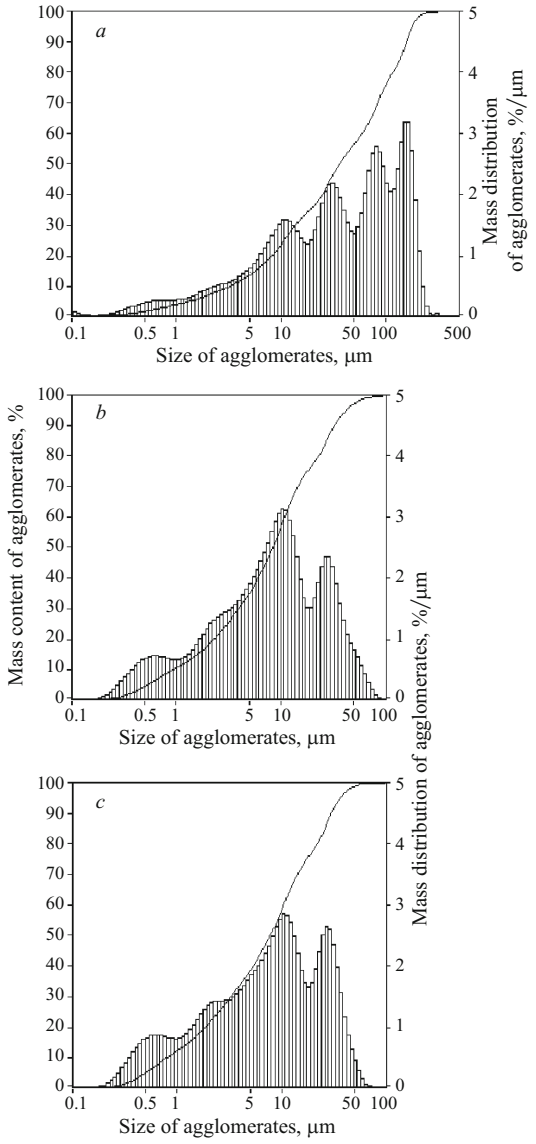

Fig. 3. Integral and differential curves of the agglomerate distribution in the synthesized powders 1/950 (*a*), 2/650 (*b*), and 3/650 (*c*).

Dense agglomerates in 3/650 powder give rise to the formation of a framework with a mixed density of the agglomerates and high (for this series of powders) closed porosity.

The differences found in the degree of structure of the powders in the system $ZrO_2 – CeO_2$, which were obtained

TABLE 3. Relative Density and Closed Porosity of Sintered Samples

Sample	Sintering temperature, °C					
	1400		1450		1500	
	ρ, %	P_{closed}, %	ρ, %	P_{closed}, %	ρ, %	P_{closed}, %
1/950	98.2	1.6	99.2	0.8	99.5	0.5
2/650	97.1	2.3	98.7	1.0	99.2	0.8
3/650	96.2	3.8	97.3	2.3	98.7	1.3

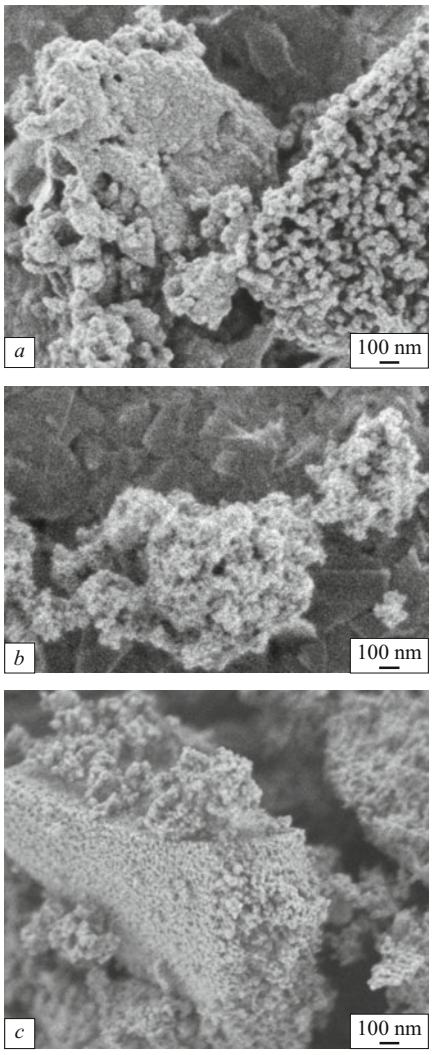

Fig. 4. Form of agglomerates in synthesized powders 1/95 (*a*), 2/65 (*b*), and 3/65 (*c*).

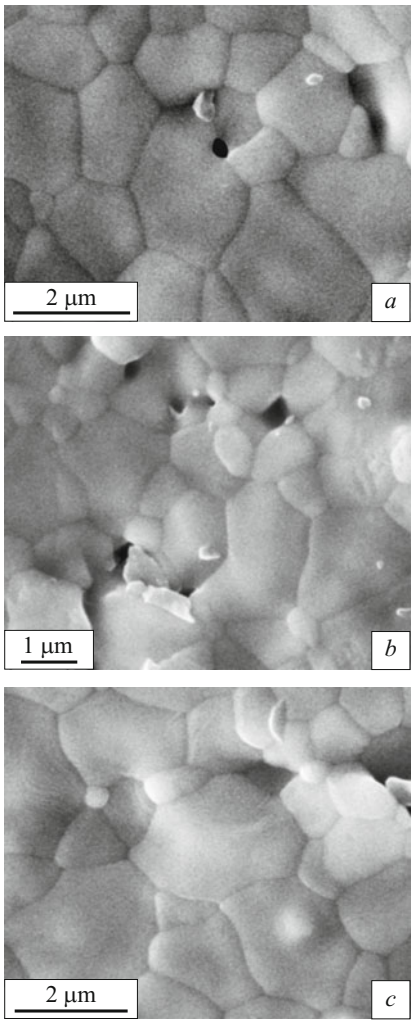

Fig. 5. Grain composition of the microstructure of a ceramic obtained from the powders 1/950 (*a*), 2/650 (*b*), and 3/650 (*c*) and sintered at 1450°C.

from carbonate and hydroxide precursors, lead to a difference in the degree of compaction of the samples.

To obtain a densely sintered ceramic from the powders developed the sintering regimes which take account of the morphological particulars of the powders, specifically, the presence of nanosize porosity which is difficult to remove, must be used.

We thank V. V. Artemov, Candidate of Physical-Mathematical Sciences and Senior Scientific Staff Member at the Institution of the Russian Academy of Sciences "A. V. Shubnikov Institute of Crystallography of the Russian Academy of Sciences" for providing the electronic photographs of the powder agglomerates.

REFERENCES

1. Ya. E. Geguzin, *The Physics of Sintering* [in Russian], Nauka, Moscow (1984).
2. V. S. Bakunov, A. V. Belyakov, E. S. Lukin, and U. Sh. Shayakhmetov, *Oxide Ceramic: Sintering and Creep* [in Russian], RKhTU, Moscow (2007).
3. V. S. Bakunov and E. S. Lukin, "Particulars of the technology of high-density technical ceramics. Aggregation of particles of the initial powders," *Steklo Keram.*, No. 3, 15 – 19 (2008); V. S. Bakunov and E. S. Lukin, "Features of high-density industrial ceramics technology. Aggregation of particles of the initial powders," *Glass Ceram.*, **65**(3 – 4), 79 – 83 (2008).
4. E. S. Lukin, "Modern high-density oxide ceramic with a regulatable microstructure. Pt. I. Effect of aggregation of oxide powders on sintering and microstructure of ceramic," *Ogneup. Tekh. Keram.*, No. 1, 5 – 14 (1996).
5. A. A. Il'icheva, S. V. Kutsev, L. I. Podzorova, et al., "Morphological particulars of nanopowders of the system Al_2O_3 – ZrO_2 – CeO_2 as a function of the conditions required to obtain the precursors," *Steklo Keram.*, No. 10, 26 – 29 (2009); A. A. Il'icheva, S. V. Kutsev, L. I. Podzorova, et al., "Morphological properties of nanopowders of the system Al_2O_3 – ZrO_2 – CeO_2 as a function of the conditions for obtaining the precursors," *Glass Ceram.*, **66**(9 – 10), 363 – 366 (2009).

6. L. I. Podzorova, A. A. Il'icheva, N. A. Mikhailina, et al., "Investigation of homogeneous precipitation of zirconium dioxide stabilized by yttrium oxide," *Ogneupory*, No. 6, 2 – 5 (1995).
7. V. Ya. Shevchenko, V. B. Glushkova, and T. I. Panova, "Production of ultradisperse powders of tetragonal solid solution in the system $ZrO_2 – Ce_2O_3$," *Neorg. Mater.*, **37**(7), 821 – 827 (2001).
8. A. A. Yashima, A. Yu. Olenin, and L. I. Podzorova, "Effect of SAS on agglomeration and structure of stabilized zirconium oxide obtained by the sol-gel method," *Neorg. Mater.*, **32**(7), 833 – 837 (1996).
9. M. Yashima, H. Takashina, et al., "Low-temperature phase equilibrium by the flux method and the metastable-stable phase diagram in the ZrO_2 CeO_2 system," *J. Am. Ceram. Soc.*, **77**(7), 1869 – 1874 (1994).
10. M. M. Ristich, V. I. Trefiov, and Yu. V. Mil'man, *Structure and Mechanical Properties of Sintered Materials* [in Russian], Serbian Academy of Sciences and Engineering, Belgrad (1992).